- Technical Paper -

MESO-SCALE MECHANICAL CHARACTERISTICS OF OVEN-DRIED MORTAR SUBJECTED TO HIGH TEMPERATURE

Onnicha RONGVIRIYAPANICH[*1], Yasuhiko SATO[*2], and Withit PANSUK[*3]

ABSTRACT

Fire incident affects the mechanical properties of mortar. The prediction methods for mortar after fire are strongly needed for making a decision to deal with the fire burnt concrete structure. This paper presents an experimental and numerical study in order to obtain the mechanical characteristics of mortar after fire. Mortar prisms were subjected to the ISO 834 for three durations, and were hewed to meso-scale specimens for conducting the tests. The mechanical characteristics would be discussed.

Keywords: mortar deteriorations, mechanical characteristics, high temperature

1. INTRODUCTION

Concrete is one of the most popular construction materials because of several advantages such as the high/benefit cost ratio, ability to cast in various shapes and sizes, and non-combustible material [1]. However, the structural concrete would be deteriorated by various factors during its life span especially for fire accidents [2-6]. Fire incident is an extreme condition that can introduce a severe damage to and cause the devastating of concrete structure [7-8]. Because of its thermal conductivity, concrete is practically considered as a fireproof layer of steel reinforcements. However, the structural concrete is basically designed and built with no fireproofing systems. As a result of this, the performance of fire damaged material as well as the structure integrity must be well understood for ascertaining whether repairing, strengthening or demolishing.

Although it is widely known that cementitious material is substantially deteriorated after fire, there have been limited studies on the prediction techniques with wide range of application for obtaining the residual structural performance. To develop such models, the mechanical characteristics of fire damaged material are effective. Some previous studies [9-12], discovered that the material properties in various scale, i.e. molecular structure of cement hydrates, physical structure, and surface deterioration, have been diminished. Consequently, the classical method to evaluate the overall performance of structure may not achieve the actual damage situations in fire problem. Moreover, it has been reported in [13] that there are three main mechanisms for deterioration in high temperature, i.e. difference of thermal characteristics between mortar and coarse aggregate, the pore pressure and the decomposition of cement hydrates. Therefore, the study on meso-scale, oven-dried mortar, should be firstly made in order to prevent additional damages due to thermal mismatching between mortar and gravel, and developing pore pressure in firing.

By taking all above explanations into consideration, the aim of the present investigations is to understand the progress of in-depth material deteriorations influenced by one-directional fire exposure. In this study, the oven-dried mortar prisms whose size is 400 mm in length, 100 mm in width and thick were subjected to the ISO 834 for 30-, 60- and 90-minute. The visual observation, 3-point flexural test, and numerical approach were used to determine the mechanical characteristics of mortar. Because the developing temperature was gathered on the entire period of burning, the relationships between those mechanical properties and temperature histories that mortar was exposed to could be discussed.

2. OUTLINE OF EXPERIMENTS

2.1 Materials and Specimens

Ordinary Portland cement and normal fine aggregate that passed through a 1.70 mm mesh sieve were used. The mortar is a non-air-entraining type and was designed based on absolute volume of the material constituent in a saturated surface dry condition that has a water to cement ratio of 0.55 and a cement to sand ratio of 0.50. Mortar prisms with 100×100×400 mm^3 were casted with embedded thermocouples at 25-, 50- and 75-mm from the surface to measure the temperature gradients during the burning process. The details of the specimen can be described as shown in Figure 1. After demolding at 24 hours, specimens were cured in water for 27 days. Then, they were dried at 105 °C for 24 hours to

*1 Graduate School of Engineering, Hokkaido University, JCI Student Member
*2 Associate Prof., Division of Engineering and Policy for Sustainable Environment, Hokkaido University, Dr.E., JCI Member
*3 Associate Prof., Dept. of Civil Engineering, Chulalongkorn University, Dr.E.

release all residual free water in the capillary pores, which causes explosive spalling during fire tests, and to keep constant moisture content until the fire test date.

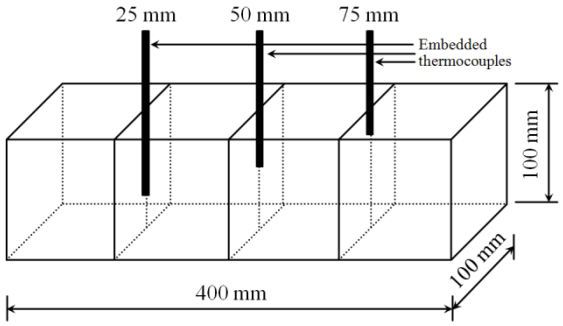

Fig.1 Specimens' details with thermocouples

2.2 Experimentations

(1) Fire simulation

The oven-dried specimens were subjected to one-directional fire exposure by being placed at the lid of a gas stove which was programmed the standard fire curve ISO 834 whose oven temperature conforms to Eq. (1). The fire tests were simulated for 30, 60 and 90 minutes in order to understand the progress of fire damage behavior of mortar.

$$T = 20 + 345\log(8t+1) \quad (1)$$

where,

T : temperature (°C)

t : elapsed time (min)

By using the embedded thermocouples and two newly installed thermocouples at heated and unheated surfaces before fire test, the developing temperature would be gathered during the entire period of burning process. The thermal gradients on cross-sectional area were, therefore, known. After reaching the target durations, the furnace would be automatically stopped, and the specimens were immediately removed and allowed to cool down in the air to ambient temperature. All damaged specimens were fully wrapped in order to prevent the additional deteriorations induced by external conditions.

(2) Flexural test

The 100×100×400 mm fire damaged specimen was cut to four of 100×100×100 mm cubes, and the internal cubes were sliced to thin specimens whose size was approximately 10 mm thick, 100 mm in length, totally 10 layers from heated to unheated sides for conducting the meso-scale flexural test. Therefore, the in-depth mechanical properties, i.e. flexural strength and modulus of elasticity, affected by uni-directional firing would be understood. Besides the visual observations on burnt mortars, the further growth of damage evidence could be also observed on both top and bottom of thin layers. The meso-scale specimens are cut from the prism specimens as shown in Figure 2.

In the test, the single point load with the constant displacement rate of 1μm/s was applied on top fiber at the center; LVDTs were placed at the mid-span and both supporting points during the entire period of testing. Therefore, the flexural strength and modulus of elasticity would be empirically calculated. The flexural strength was calculated using Eq. (2), while the modulus of elasticity was also determined based on the elastic theory as shown in Eq. (3).

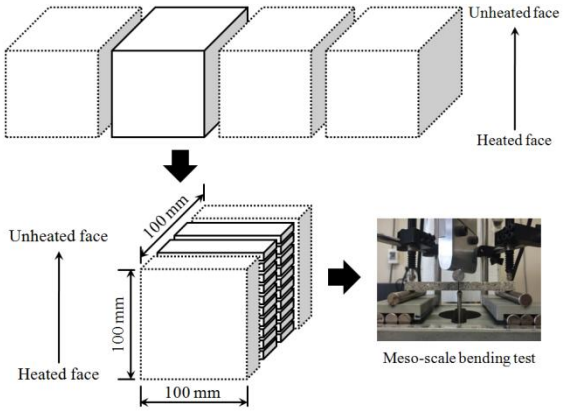

Fig. 2 Location of specimen for flexural test

$$F_b = \frac{3 \cdot P \cdot L}{2 \cdot b \cdot h^2} \quad (2)$$

$$E = \frac{P_{1/3} \cdot L^3}{4 \cdot \delta_{1/3} \cdot b \cdot h^3} \quad (3)$$

where,

F_b : Flexural strength (MPa)

E : Modulus of elasticity (MPa)

P : Peak load (N)

$P_{1/3}$: 1/3 of peak load (N)

$\delta_{1/3}$: Displacement at 1/3 of peak load (mm)

L : Span length (mm)

b, h : Section width, depth (mm)

Practically for the fire damaged series, the bending failure might not be occurred at the mid-span due to the existence of fire cracks. In that case, the flexural strength would be calculated using the actual bending moment obtained at the actual bending failure location.

(3) Multi-linear approximation method

By using the program of multi-linear approximation method, JCI-S-001-2003, the tensile strength, the fracture energy, and the tension softening curve would be obtained from the experimental load-displacement curves.

3. RESULTS AND DISCUSSION

3.1 Temperature Gradients

During the fire tests, several kinds of temperature were collected such as oven's, surfaces' and internal temperatures with embedded thermocouples. Although one face of specimen was directly exposed to fire, the temperature at heated face might not have been equal to the oven's temperature. Therefore, the temperature measured at heated face is more appropriate value to describe the developed thermal gradients and temperature background at each

depth during fire rather than the oven's temperature.

A thermal loading, in terms of the fire exposure, was applied to the heated face, which experienced a drastically increased temperature, while the temperature of the internal layer of mortar might be comparatively low. The internal temperature gradients started gradually increased with the elapsed exposure time. At the same distance from the heated side, the maximum internal temperature increases when subjected to a longer duration and gradually decreases with a greater distance from the heated face. As seen in Figure 3, the temperature's difference is larger between 0 and 25 mm from the heated face compared with its gradients at further distance in case of 30 minutes under firing. With respect to an increment of time exposure, i.e. 60 and 90 minutes under firing, the steep temperature gradients could be found within the range of less than 50 mm from heated side, while the gradients beyond that front are similar to 30 minutes firing. It was probably said that, the heat transportation through cementitious material proceed gradually due to its thermal conductivity. In addition, the initiation and propagation of crack introduced by fire exposure [9] and crack intensity may cause the non-uniform temperature gradient along the cross section [14]. According to the Eurocode, the mechanical strength tends to decrease with various maximum temperatures. Therefore, the mechanical characteristics at each depth especially for the first half of section thickness are probably high variant compared with the location beyond 50 mm from burning sides in which the temperature gradients were relatively flat.

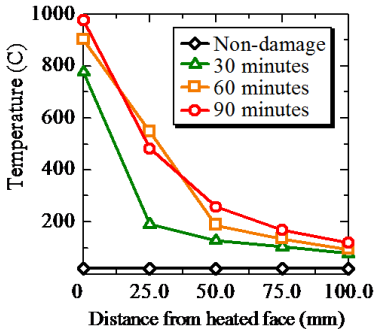

Fig. 3 Maximum temperature at each depth

3.2 Post-fire Crack Assessments

This task may not aim at to quantify the fire damage evidences, but to demonstrate the general specimens' conditions after fire. By means of surface observations, there are two types of cracks observed on the directly heated surface, and 100×400 mm^2 long side faces of mortar prisms.

Figure 4 indicates the crack characteristics after heating and cooling regimes. During exposure to fire, the heated face started cracking with interconnection between cracks, then crazing was found on the heated face in all the fire cases. Because the specimens were allowed to cool down immediately after reached the target durations, the heated face which was expanded in heat was suddenly shrunk leading to the relatively straight cracking on long sides. In addition, cracking on the side face was probably interconnected with the heated surface's crazing at the border. This means that some of the damage evidences may affect the material strength in serviceability level.

(a) 30 minutes under firing

(b) 60 minutes under firing

(c) 90 minutes under firing

(d) Heated face (90 minutes under firing)

Fig. 4 Crack patterns on specimens

3.3 Flexural Strength and Modulus of Elasticity

The flexural strength for all fire damaged series and control specimens is illustrated in Figure 5. The average flexural strength of non-damaged mortar is 7.16 N/mm^2, while the reduction tendency was clearly indicated in all of the fire cases especially for the layer that was directly burnt at the bottom. The flexural strength of those layers was reduced for 66%, 72% and 81% of non-damaged strength for 30, 60 and 90 minutes under firing, respectively. The loss of flexural strength of those layers is not significantly different in all fire cases because it is depending on the bending failure location where the crack propagated from the crazing might exist. That kind of crack is found up to approximately 20 mm for 30 minutes under firing, and 40 mm from heated side in case of 60 and 90 minutes under firing. At the greater distance from heated surface, the flexural strength is increased and became similar to the flexural strength of non-damaged material. However, the slightly increment in strength could be also observed in some layers next to the severe damaged zone. It is probably because of the rehydration of the unhydrated cement particles within the appropriate range of temperature.

In the flexural test, the bending failure mode could be divided into two categories as shown in Figure 6. The notch was set at the mid-span of all thin

specimens. When applying a single point load at the top fiber up to the load limit, the real crack would occur. Practically, some thin specimens might contain the major crack such as the specimens in the severe damaged zone. In that case, a bending failure location was depending on the fire crack location. Figure 6(a) shows the bending failure location which has been randomly found in various locations outside the notch at the mid-span. On the other hand, the bending crack of the non-damaged specimen and the specimen without the visible crack was usually found at the preexisting crack, as shown in Figure 6(b).

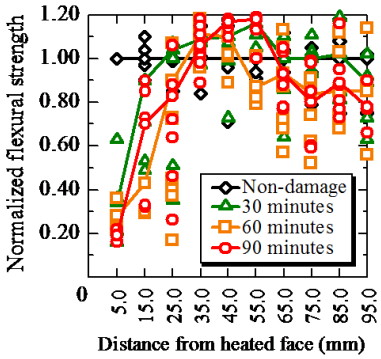

Fig. 5 In-depth meso-scale flexural strength

(a)

(b)

Fig. 6 Schematic of bending failure location

In addition to the flexural strength, the modulus of elasticity could be also obtained. Figure 7 shows the average in-depth modulus of elasticity. The result shows that the severe damaged zone could be observed as same as the flexural strength. When the distance moves farther from the heated side, the modulus of elasticity would be increased. However, it was supposed to be decreased with thermal experiences from the non-damaged specimen.

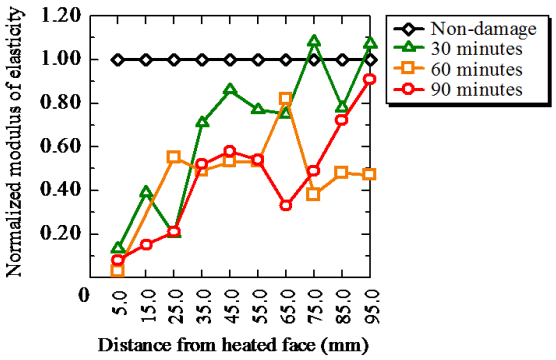

Fig. 7 In-depth modulus of elasticity

3.4 Tensile Strength and Fracture Energy

The observed load-displacement curves could be used for obtaining the tensile strength by using the multi-linear approximation method of JCI-S-001-2003. However, those experimental data must be gathered from the specimens whose bending failure is only at the preexisting crack. Therefore, the load-displacement of thin with existing fire crack might not be able to use for obtaining the tensile strength by this technique.

Figure 8 shows the average in-depth tensile strength of all fire cases including reference series. The average tensile strength of non-damaged specimens is 4.99 N/mm^2. However, the tensile strength of all burnt series was also similar to non-damaged specimen. It could be said that those burnt specimens did not contain any major cracks, and might be similar to non-damage one. As a result of this, the existence of crack could have an influence on mechanical characteristics in the fire problem of cementitious material.

As widely known, the tensile strength should have a same tendency with the flexural strength. This study also shows the good agreement between those two mechanical properties in the zone that properties were recovered. From the location where the flexural strength is similar to non-fired material onwards, the tensile strength is also observed the same trend. Consequently, the tensile strength in severe damaged zone which could not be obtained in this study may have a same residual proportion with the loss in flexural strength.

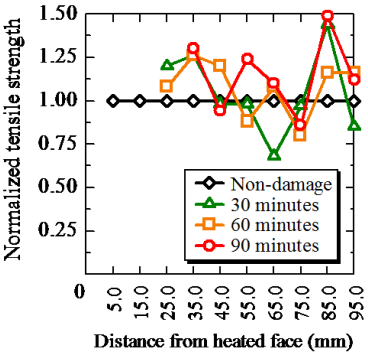

Fig. 8 In-depth tensile strength

The fracture energy would be calculated from the area under tensile stress-crack width curves. The examples of tension softening curves obtained from multi-linear approximation technique are illustrated in Figure 9(a) to 9(d). They show the tension softening curves obtained at 35.0 mm, 45.0 mm, 55.0 mm and 65.0 mm from heated face, respectively. Because the relations of tensile stress-crack width are approximately same, the calculated fracture energy was not significantly different among all specimens including control set.

Besides the technique of JCI-S-001-2003, the fracture energy could be also determined following the recommendation of RILEM [15]. Based on this method, the fracture energy could be calculated using

the specimens' details and the load-displacement curves as shown in Eq. (4) and Eq. (5).

$$G_f = \frac{W_0 + W_1}{A_{lig}} \quad (4)$$

$$W_1 = \left(\frac{L_s}{L} \cdot m_1 + 2 \cdot m_2\right) \cdot N \cdot \delta_{tu} \quad (5)$$

where,

G_f : fracture energy (N/m)
W_0 : area under P-δ curve (N-mm)
A_{lig} : cross sectional area at mid-span (mm^2)
L_s : length of specimen (mm)
L : span length (mm)
m_1 : specimen's dead weight (g)
m_2 : weight of all equipments (g)
N : gravitational acceleration (m/s^2)
δ_{tu} : displacement at 2 N (mm)

By using those two techniques for determining the fracture energy, the comparison is shown in Figure 10. Both approaches are completely good agreement.

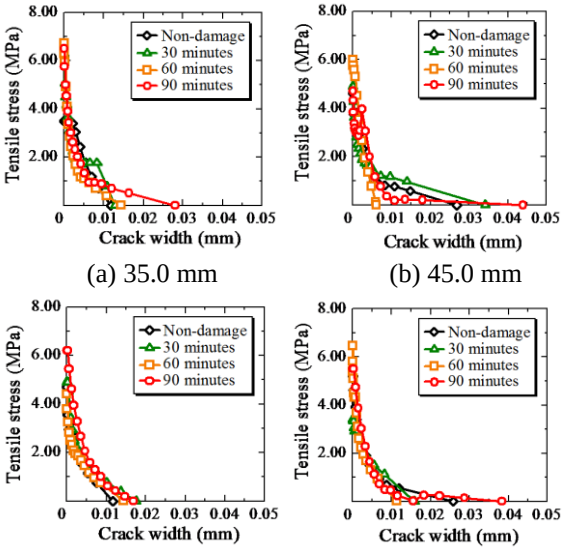

(a) 35.0 mm (b) 45.0 mm

(c) 55.0 mm (d) 65.0 mm

Fig. 9 Tensile stress-crack width curves (At various distances from heated face)

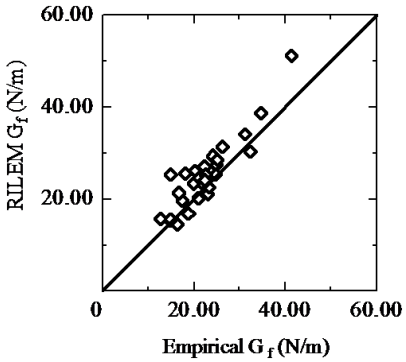

Fig. 10 Fracture energy using JCI and RILEM

3.5 Change of Mechanical Characteristics

Although the material properties-temperature experience had a relationship, this study has discovered that the existence of crack might play more prominent role on the material behavior of cementitious material in fire problem.

According to the post-fire material behavior in this study, the damaged specimens with no existing visible crack were almost similar to non-thermal experienced one. In order to obtain the better understanding about the actual post-fire properties of mortar, the influence of temperature experience as well as the significance of crack initiated by fire should be taken into account.

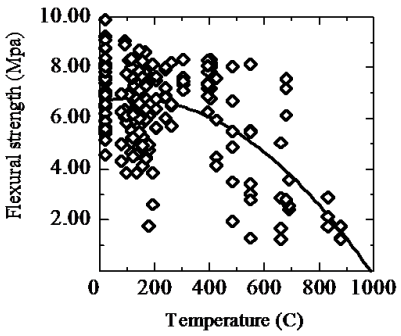

Fig. 11 Flexural strength-temperature relation

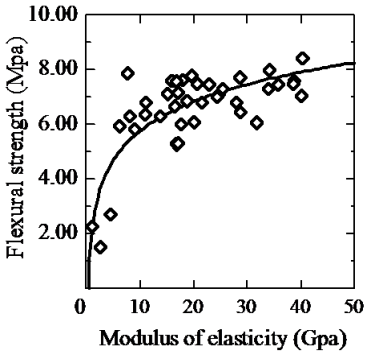

Fig. 12 Flexural strength-modulus of elasticity

Figure 11 shows the relationship between flexural strength and temperature. The regression line was constructed based on the existing knowledge about the regenerated and decomposition of chemical compounds at elevated temperature. At the early stage of burning process, the hydration process could be regenerated within an appropriate range of temperature. After that, the decomposition would be taken place. Therefore, the flexural strength with heat treatment is slightly increased from the strength without any damages background and the rapidly decreasing tendency is observed. With respect to an increment of temperature, the flexural strength would be more scattering because of the influence of existing fire crack. Meanwhile, Figure 12 shows the relationship between modulus of elasticity and flexural strength. The obviously decreased in the modulus of elasticity could be found in case the flexural strength was also comparatively low, i.e. the flexural strength of the specimens in severe damaged zone containing fire crack. In case of the burnt specimens without fire crack, the modulus of

elasticity was also decreased even though the flexural strength was similar to non-damage material.

Since the performance of mortar would be substantially diminished especially for the specimens with major cracks, the precise material model to achieve the mechanical properties of fire damaged cementitious material must consider the effect of cracking induced by fire exposure.

4. CONCLUSIONS

(1) A thermal loading, in term of fire exposure, applied to one surface could develop the internal temperature history leading to the attenuation of cementitious material's properties. With an increment of exposure duration, the progresses of temperature were strongly related to the level of material deteriorations especially in the severe damaged zone.

(2) In severe damaged specimens, the existing crack induced by fire would be a weak point which clearly affects the failure mode in flexural test. In addition, the material strength of the specimen with visible crack would be also obviously diminished. Meanwhile, the similarity to non-damaged material of the strength would be observed beyond the severe damaged region.

(3) The temperature effect with considering the crack initiated by fire exposure is the appropriate index to achieve the actual mechanical characteristics of fire damaged cementitious material.

ACKNOWLEDGEMENT

The authors gratefully acknowledge the Hokkaido Northen Regional Building Research Institute in Asahikawa, Japan that supported the fire furnace in this study.

REFERENCES

[1] Siam Cement Group, Co., Ltd. "Cement and Applications." ISBN 974-92652-4-6, 2009. (in Thai)

[2] Xu, Y., Wong, Y. L., Poon, C. S., and Anson, M., "Impact of high temperature on PFA concrete," Cement and Concrete Research, Vol. 31, 2001, pp. 1065-1073.

[3] Husem, M., "The effects of high temperature on compressive and flexural strengths of ordinary and high-performance concrete," Fire Safety Journal, Vol. 41, 2006, pp. 155-163.

[4] Vichit-Vadakan, W. and Elizabeth, A. K., "Transport properties of fire-exposed concrete," Journal of Advanced Concrete Technology, Vol. 7, 2009, pp. 393-401.

[5] Belkacem, T., and Musa, R., "Influence of high temperature on surface cracking of concrete studied by image scanning technique," Jordan Journal of Civil Engineering, Vol. 4, 2010, pp. 155-163.

[6] Sato, Y., Miura, T., and Nakamura, H., "Meso-scale analysis of the mechanical properties of chemically-deteriorated mortar," The 10th International conference on mechanics and physics of creep, shrinkage, and durability of concrete and concrete structures, 2015, Vienna, Austria, pp. 1251-1258.

[7] Heikal, M., "Effect of temperature on the physico-mechanical and mineralogical properties of Homra pozzolanic cement pastes," Cement and Concrete Research, Vol. 30, 2000, pp. 1835-1839.

[8] Rongviriyapanich, O., Pansuk, W., and Sato, Y., "Effect of chemical compound reduction on oven-dried mortar subjected to elevated temperature," The 18th National Convention on Civil Engineering, 2013, Chiangmai, Thailand.

[9] Arioz, O., "Effects of elevated temperature on properties of concrete," Fire Safety Journal, Vol. 42, 2007, pp. 516-522.

[10] Piasta, J., Sawicz, Z., and Rudzinki, L., "Changes in the structure of hardened cement paste due to high temperature," Material Construction, Vol. 17, 1984, pp. 291-296.

[11] Lin, W. M., Lin, T. D. and Powers-Couche, L. J., "Microstructures of fire-damaged concrete," ACI Materials Journal, 1996, pp. 199-205.

[12] Peng, G. F., and Huang, Z. S., "Change in microstructure of hardened cement paste subjected to elevated temperatures," Construction and Building Materials, Vol. 22, 2008, pp. 593-599.

[13] Fu, Y. F., Wong, Y. L, Poon, C. S., Tang, C. A., and Lin, P., "Experimental study of micro/macro crack development and stress-strain relations of cement-based composite materials at elevated temperatures," Cement and Concrete Research, Vol. 34, 2004, pp. 789-797.

[14] Abdulkaremm, O. A., Mustafa Al Bakri, A. M., Kamarudin, H., Khairul Nizar, I., and Saif, A. A., "Effects of elevated temperatures on the thermal behavior and mechanical performance of fly ash geopolymer paste, mortar and lightweight concrete," Construction and Building Materials, Vol. 50, 2014, pp. 377-387.

[15] RILEM Draft Recommendation, "Determination of the fracture energy of mortar and concrete by means of three-point bend tests on notched beams materials and structures," Vol. 18, 1985, pp. 285-290.

[16] Bazant, P. Z., and Chern, J. C., "Stress-induced thermal and shrinkage strains in concrete," ASCE Journal of Engineering Mechanics, Vol. 113, pp. 1493-1511.

[17] Chang, Y. F., Chen, Y. H., Sheu, M. S., and Yao, G. C., "Residual stress-strain relationship for concrete after exposure to high temperatures," Cement and Concrete Research, Vol. 36, 2006, pp. 1999-2005.